Proceedings of CONF-FMCE 2025 Symposium: AI and Machine Learning Applications in Infrastructure Engineering
DOI: 10.54254/2755-2721/2025.MH26314

Optimization Design of Doping Concentration and Fiber Length for Thulium-Doped Fiber Lasers

Yi Sun

School of Physical Science and Technology, Nantong University, Nantong, China
2202110102@stmail.ntu.edu.cn

Abstract. This paper focuses on the optimization design of thulium-doped fiber lasers in the L+ band (1600-1650nm). Aiming at the problem of low output power and efficiency in this band, it takes silicon-based thulium-doped fiber as the gain medium and studies the influence of parameters such as doping concentration and fiber length on the steady-state characteristics of the laser by establishing a coupled model of three-level rate equations and transmission equations. The simulation results show that there is an optimal combination of parameters: when the doping concentration is about $3\times10^{24}/m^3$ and the fiber length is about 0.4m, the laser has a threshold of about 0.04W, the highest pumping efficiency, and the output power increases linearly with the pumping power. The research also provides theoretical support for the experimental preparation of thulium-doped fiber lasers in the L+ band and looks forward to their application prospects in biomedical, industrial processing and other fields.

Keywords: Thulium-Doped Fiber Laser(TDFL), L+ band, doping concentration, fiber length

1. Introduction

The output capability of thulium-doped fiber lasers in the L+ band (1600-1650nm) has a profound impact on the development of modern science and technology. In the biomedical field, this wavelength band lies within the eye-safe spectral range (>1400nm) and can be used for non-invasive surgery and high-precision tissue ablation; in the field of communications, it is compatible with the low-loss window (U-band) of existing silica fibers, providing a new type of light source for high-rate communications; in the field of lidar, it can improve atmospheric penetration and optimize the accuracy of environmental monitoring; in the field of material processing, it can achieve precise processing of polymers. In addition, the L+ band is located near the strong water absorption peak (~1940nm), which offers unique advantages for humidity-sensitive gas sensing. Therefore, breaking through the long-wavelength output limit of thulium-doped fiber lasers is not only an important extension of fiber laser technology, but also will promote technological innovation in interdisciplinary applications.

In recent years, thulium-doped laser technology has developed rapidly, with research focusing on gaining medium design, pump mechanism optimization, and wavelength extension. Wang Jianwei et al. constructed an experimental setup of a 793nm directly pumped broadband tunable narrow-

DOI: 10.54254/2755-2721/2025.MH26314

linewidth ring cavity 2μm thulium-doped fiber laser, which is used to achieve narrow-linewidth laser output with tunable wavelength in the 2μm band [1]. Researchers Yan et al. from the Laser Research Institute have developed a 1950nm narrow-linewidth, high-peak-power nanosecond pulsed fiber laser [2]. Gutty et al. from France constructed a tunable pulsed thulium-doped fiber laser using the active Q-switching method. This laser adopts 1550nm laser as the pumping light for core pumping and uses an AOM (Acousto-Optic Modulator) as the Q-switch for modulation, achieving nanosecond pulsed output with tunable wavelengths in the range of 1860-1960nm [3]. Samion et al. constructed a tunable pulsed fiber laser operating in the 1.9μm band, which uses a thin film based on multi-walled carbon nanotubes as a saturable absorber for passive Q-switching [4]. Zhou Renlai et al. used a 1.558μm pulsed laser as the pump source to construct an all-fiber gain-switched thulium-doped pulsed fiber laser [5]. Zhang H R et al. reported a gain-modulated thulium-doped all-fiber oscillator directly pumped by a pulsed semiconductor laser, with a pump wavelength of 793nm and an output pulse center wavelength of 2017nm [6]. Tang et al. reported a tunable thulium-doped fiber laser with a linear cavity structure, where the output wavelength can be changed by adjusting the reflectivity of the output mirror and the length of the thulium-doped fiber. By varying the reflectivity of the output mirror, wavelength tuning in the range of 1949~2055 nm can be achieved, and a maximum output power of 32 W is obtained at 1949 nm [7]. Cheng Xi et al. from the National University of Defense Technology constructed a 2μm all-fiber tunable thulium-doped pulsed laser based on gain switching. This laser uses a 1550nm laser as the pump light, and another 1550nm pulsed laser as the gain switch of the system. The repetition frequency of this pulsed laser is tunable in the range of 1kHz-2MHz, and the pulse width is tunable in the range of 10-200ns [8]. Du Gego et al. achieved continuous-wave laser output using a double-clad thulium-doped fiber laser at room temperature. The laser employs a 791nm wavelength semiconductor laser for cladding pumping, with a slope efficiency of 50%, delivering 6W of continuous-wave laser at a wavelength of 2μm [9]. In 2017, G. A. Newburgh et al. used an LD with an output wavelength of 1620 nm to directly pump a thulium-doped fiber laser. They successfully achieved a laser output of 15 W with a slope efficiency as high as 67% [10]. However, existing research still lacks parameter optimization models for systematic design in the 1600-1650nm band, and the output power and efficiency are generally lower than those in the short-wavelength region.

This study focuses on the systematic design of thulium-doped fiber lasers in the L+ band (1600-1650 nm). Silicon-based thulium-doped fiber is selected as the gain medium, with emphasis on addressing the key limiting factors for long-wavelength output. First, a dynamic model of thulium ion transitions is established to quantify the effects of pump wavelength, doping distribution, and fiber geometric parameters on population inversion. Second, the correlation mechanism between the lifetime of the upper energy level ($^3F_4$) and matrix polarity is studied. Finally, a complete coupled model of steady-state rate equations and transmission equations is constructed to realize the collaborative regulation of pump absorption, excited state transfer, and wavelength competition behavior. The core objective of the research is to determine the optimal parameter combination for breaking through the 1600nm output limit, covering elements such as pump power threshold, doping concentration, fiber length, and end-face reflectivity.

2. Theoretical basis and research methods

2.1. Basic principles of lasers and three-level systems

The working principle of thulium-doped fiber lasers is based on the three-level system of thulium ions (Tm^{3+}). The energy level structure and transition process of this system form the basis for

DOI: 10.54254/2755-2721/2025.MH26314

understanding its operating mechanism. In a three-level system, thulium ions have three main energy levels, namely the ground state energy level N_0, the excited state energy level N_1, and the upper energy level N_3. When pump light irradiates the thulium-doped fiber, thulium ions in the ground state energy level absorb the energy of the pump light and thus transition to the upper energy level. Subsequently, the ions in the upper energy level transfer to the excited state energy level through a non-radiative relaxation process, and when the ions in the excited state energy level transition back to the ground state, laser light is emitted.

It can be derived from the energy level transitions of thulium ions that the energy level transitions of thulium ions involve multiple wavelength bands. Among them, the transition from the ground state energy level $^3H_6$ to the upper energy level $^3H_4$ corresponds to a pump light wavelength of approximately 793 nm, while the transition from the excited state energy level $^3F_4$ to the ground state energy level $^3H_6$ can generate laser light in wavelength bands such as around 1630 nm and around 2000 nm, which is also related to the research scope of the L+ band (1600-1650 nm).

The absorption spectrum of thulium ions exhibits their absorption characteristics at different wavelengths. Within the wavelength range of 400-2000 nm, there are multiple absorption peaks. Among them, the absorption peak corresponding to the $^3H_6 \rightarrow {}^3H_4$ transition is around 790 nm, and this wavelength band has the largest absorption cross-section, so semiconductor lasers can be used for pumping to achieve good results. In addition, there are absorption peaks corresponding to transitions such as $^3H_6 \rightarrow {}^3H_5$ (around 1210 nm), $^3H_6 \rightarrow {}^3F_3$, $^3H_6 \rightarrow {}^3F_4$, and $^3H_6 \rightarrow {}^1G_4$. The emission spectrum of thulium ions shows that their emission wavelength range in silica fiber is from 1600 nm to 2200 nm, which also provides the possibility for laser output in the L+ band (1600-1650 nm).

The transition process of the three-level system is affected by various factors, such as pump light power, doping concentration, and fiber length. Through research on the three-level system, we can conduct in-depth analysis of key parameters such as the gain characteristics and threshold conditions of the laser, which provides a basis for further optimizing the performance of thulium-doped fiber lasers.

2.2. Rate equations

To describe the energy level transitions of ions and the photon generation process in thulium-doped fiber lasers, a rate equation model is established. The rate equations mainly include mathematical descriptions of processes such as pump light absorption, excited state transitions, spontaneous emission, and stimulated emission.

For a three-level system, the rate equations can be expressed as:

$$\frac{\partial N_1(z)}{\partial t} = -\left[W_p(z) + W_{12}(z)\right]N_1(z) + A_{21}N_2(z) + W_{21}(z)N_2(z) \tag{1}$$

$$\frac{\partial N_2(z)}{\partial t} = W_{12}\left(z\right)N_1\left(z\right) - W_{21}\left(z\right)N_2\left(z\right) - A_{21}N_2\left(z\right) + A_{32}N_3\left(z\right) \tag{2}$$

$$\frac{\partial N_3(z)}{\partial t} = W_p\left(z\right)N_1\left(z\right) - A_{32}N_3\left(z\right) \tag{3}$$

$$N = N_1(z) + N_2(z) + N_3(z) \tag{4}$$

DOI: 10.54254/2755-2721/2025.MH26314

W_p, W_{12}, W_{21}, A_{32}, and A_{21} are the pump light absorption rate, signal light absorption rate, signal light stimulated emission rate, respectively, with the unit all being s^{-1}.

$$\begin{aligned} W_p(z) &= \frac{\sigma_{13}P_p(z)}{h\nu_{13}A_{\text{eff}}} \\ W_{12}(z) &= \frac{\sigma_{12}(\nu_{12})P_s(z)}{h\nu_{12}A_{\text{eff}}} \end{aligned} \tag{5}$$

$$W_{21}(z) = \frac{\sigma_{21}(\nu_{21})P_s(z)}{h\nu_{21}A_{\text{eff}}} \tag{6}$$

$$A_{\text{eff}} = \pi r^2 \tag{7}$$

2.3. Power propagation equations

In thulium-doped fiber lasers, the propagation of optical power follows the power propagation equation. This equation takes into account factors such as absorption, gain, and loss of light in the fiber, and is used to describe the propagation characteristics of pump light and signal light in the fiber.

The power propagation equation can be expressed as:

$$\frac{\mathrm{d}P_p^+(z)}{\mathrm{d}z} = -(\Gamma_p\sigma_{ap}N + \alpha_p)P_p^+(z) \tag{8}$$

$$\frac{\mathrm{d}P_p^-(z)}{\mathrm{d}z} = \left(\Gamma_p\sigma_{ap}N + \alpha_p\right)P_p^-\left(z\right) \tag{9}$$

$$\frac{\mathrm{d}P_s^+(z)}{\mathrm{d}z} = [\Gamma_s(\sigma_{es} + \sigma_{as})N_{32} - \Gamma_s\sigma_{as}N - \alpha_s]P_s^+(z) \tag{10}$$

$$\frac{\mathrm{d}P_s^-(z)}{\mathrm{d}z} = -[\Gamma_s(\sigma_{es} + \sigma_{as})N_{32} - \Gamma_s\sigma_{as}N - \alpha_s]P_s^-(z) \tag{11}$$

And then the threshold power is obtained.:

$$P_{\text{th}} = \frac{\left(NT_s\sigma_{as} + \alpha_s\right)L + \ln\left(\frac{1}{\sqrt{R_1R_2}}\right)}{\frac{1-\exp(\beta)}{v_p}} \cdot \frac{v_s}{v_p} \cdot P_{\text{ssat}} \tag{12}$$

DOI: 10.54254/2755-2721/2025.MH26314

3. Simulation results

3.1. Investigation on the steady-state characteristics of thulium-doped fiber lasers

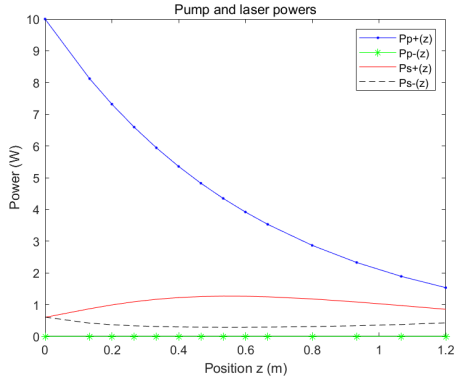

Figure 1. Diagram of optical power transmission law

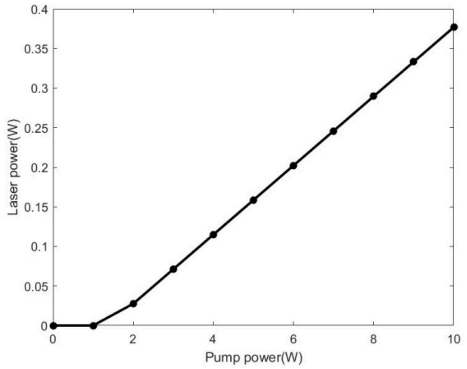

Figure 2. Diagram of output characteristics of fiber laser

Figure 1 is a diagram of the optical power transmission law. As shown in Figure 2, the thulium-doped fiber laser exhibits obvious threshold characteristics. When the pump power is low (approximately less than 1W), the laser power is almost zero, failing to reach the lasing threshold, and the gain cannot overcome the loss to achieve laser output. However, when the pump power exceeds the threshold (approximately 1W), the laser power increases approximately linearly with the increase of pump power. At this time, the gain medium effectively realizes population inversion and can convert the pump energy into laser output. In terms of the distribution of optical power along the fiber length, as shown in Figure 1, the forward pump light (Pp+(z)) continuously attenuates from the input end (z=0) to the output end (z=1.2m) of the fiber, which reflects the process in which the pump light is absorbed by the gain medium in the fiber for population inversion. The power of the backward pump light (Pp-(z)) is approximately zero and remains stable, indicating that the pump is mainly injected in the forward direction and effectively absorbed. The forward signal light (Ps+(z)) first increases and then decreases slightly. In the initial stage, the signal light is amplified because the gain is greater than the loss. Later, due to the attenuation of the pump light and changes in the population inversion degree of the gain medium, the growth slows down or even drops slightly. The power of the backward signal light (Ps-(z)) is low and stable. Due to the limited reflectivity of the output mirror (R2=0.5), the backward feedback is weak, and the output is mainly forward laser light.

DOI: 10.54254/2755-2721/2025.MH26314

3.2. Investigation on the influence of doping concentration on the steady-state characteristics of fiber lasers

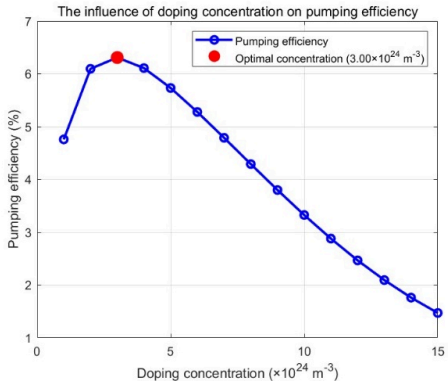

Figure 3. Curve of the relationship between doping concentration and pumping efficiency

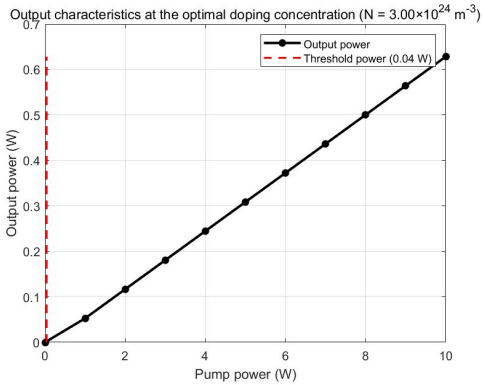

Figure 4. Diagram of output characteristics under optimal doping concentration

When investigating the influence of doping concentration on the steady-state characteristics of fiber lasers, it is found that, as shown in Figure 4, there exists an optimal doping concentration at which there is a clear threshold (approximately 0.04 W). Meanwhile, as shown in Figure 3, the influence of doping concentration on pumping efficiency is characterized by the existence of an optimal value (3.00×10^{24} m^{-3}). When the concentration is lower than this value, the pumping efficiency increases with the increase of concentration, because more thulium ions participate in stimulated emission, and the gain is improved. When the concentration is higher than this value, the efficiency decreases continuously with the increase of concentration. This may be due to the intensified energy transfer loss between ions at high concentrations or gain saturation, which leads to the reduction of the efficiency of converting pump energy into laser output. For potential optimization points, we can consider exploring the uniformity of concentration distribution and simulating the influence of gradient concentration on efficiency.

DOI: 10.54254/2755-2721/2025.MH26314

3.3. Investigation on the influence of fiber length on the steady-state characteristics of fiber lasers

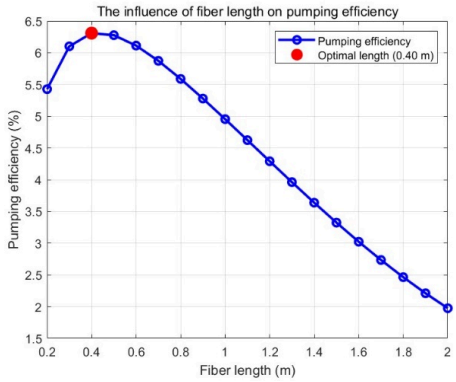

Figure 5. Curve of the relationship between fiber length and pumping efficiency

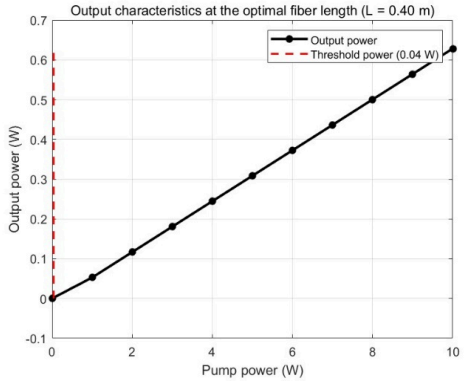

Figure 6. Diagram of output characteristics under optimal fiber length

Regarding the influence of fiber length on the steady-state characteristics of fiber lasers, as shown in Figure 6, the study indicates that there exists an optimal fiber length, at which there is a clear threshold (0.04 W). The influence of fiber length on pumping efficiency also has an optimal value (0.40 m), as shown in Figure 5. When the length is less than the optimal value, the pumping efficiency increases with the increase of length. This is because a longer fiber provides more gain medium, extends the interaction distance between light and particles, and promotes the absorption and conversion of pump energy. When the length exceeds the optimal value, the efficiency decreases continuously with the increase of length. This is due to the accumulation of losses (such as scattering and absorption losses) caused by an excessively long fiber, and may also lead to problems such as gain saturation, thereby reducing the conversion efficiency of pump energy into laser output. Potential optimization points can explore length gradient design, such as adopting segmented doping of gain fibers to balance the gain and loss in different regions.

Through the systematic research on thulium-doped fiber lasers, it is concluded that their key parameters (such as doping concentration and fiber length) need to be optimized synergistically. These parameters each have their own optimal values. When the doping concentration is approximately $3\times10^{24}/m^3$ and the fiber length is about 0.4m, the pumping efficiency is the highest, the threshold is low (around 0.04W), the output power increases linearly with the pump power, and the energy conversion is stable. This is because a reasonable doping concentration combined with an

DOI: 10.54254/2755-2721/2025.MH26314

appropriate fiber length can enable the pump light to be fully absorbed in the fiber, while avoiding the impact of adverse factors such as ion clustering, thereby achieving the optimal performance of the laser. In addition, the laser has a clear threshold. When the pump power is lower than the threshold, there is no effective output; when it is higher than the threshold, the output power has a linear relationship with the pump power, which reflects a stable balance between gain and loss. This characteristic indicates that above the threshold, the laser operates in a relatively stable state, and its energy conversion capability can be evaluated by the slope efficiency.

In terms of application prospects, thulium-doped fiber lasers can be used for optical coherence tomography (OCT) imaging in the biomedical field. Taking advantage of the penetration depth and resolution characteristics of light in this wavelength band, they can achieve high-resolution imaging of the internal structure of biological tissues, providing more accurate information for disease diagnosis. They can also be combined with photothermal/photodynamic effects for the treatment of skin diseases. By precisely controlling the energy and wavelength of the laser, the photothermal effect can be used to destroy diseased tissues, or the photodynamic effect can be used to activate photosensitizers, selectively killing diseased cells and reducing damage to normal tissues. In the field of industrial processing, it can provide stable medium and high power output for thin-plate metal welding and precision cutting. By virtue of its high energy density and precise control capability, it can achieve efficient and low-deformation processing effects, meeting the requirements for processing accuracy and quality in the field of high-end manufacturing.

In the future, its performance can be further optimized through innovations in optical fiber materials and exploration of new structures and gain media, such as exploring new host materials like fluoride glass. Fluoride glass can inhibit the non-radiative transition of thulium ions and prolong the lifetime of the upper energy level, thereby improving the gain efficiency. Chalcogenide glass has a wide infrared transmission range, which can optimize the transmission loss of 1640nm signal light, reduce energy loss, and improve the output power and efficiency of the laser. In addition, the adoption of a double-clad fiber structure can expand the absorption area of the pump light and improve the utilization efficiency of the pump light, thereby increasing the output power of the laser. Research on the modification of thulium ion-doped substrates to regulate the luminescent properties of ions can further enhance the performance of the laser, such as broadening the gain bandwidth and improving wavelength stability. Through these methods, it is expected to achieve laser output with higher power and higher efficiency in the L+ band, promoting the wide application of thulium-doped fiber lasers in various fields.

4. Conclusion

This paper focuses on thulium-doped fiber lasers in the L+ band (1600-1650 nm). Using silicon-based thulium-doped fiber as the gain medium, it studies the influence of parameters such as doping concentration and fiber length on the steady-state characteristics of the laser by establishing a coupled model of three-level rate equations and transmission equations. The simulation shows that the laser has a threshold characteristic: when the pump power exceeds the threshold, the output power increases linearly. The forward pump light attenuates along the fiber, while the forward signal light first increases and then decreases. The optimal parameters are a doping concentration of $3\times10^{24}/m^3$ and a fiber length of 0.4 m, at which point the threshold is approximately 0.04 W and the pumping efficiency is the highest.

This research provides theoretical support for the experimental preparation of thulium-doped fiber lasers in the L+ band. It has broad application prospects in fields such as biomedicine and industrial processing. In the future, performance can be optimized by exploring new host materials

DOI: 10.54254/2755-2721/2025.MH26314

such as fluoride glass and adopting double-clad structures. It is expected to achieve output with higher power and efficiency, promoting technological innovation and application expansion in multiple fields.

References

[1] Wang, J.W., Shen, H., Ren, J.J., et al. (2025) 793 nm Directly Pumped Broadband Tunable Narrow-Linewidth Ring Cavity 2 μm Thulium-Doped Fiber Laser. Laser & Optoelectronics Progress, 62, 1314001.
[2] Yan, W., Sun, S., Wang, L., et al. (2021) High-Performance Narrow-Linewidth Nanosecond Pulsed Fiber Laser in 2 μm Band. Seventh Symposium on Novel Photoelectronic Detection Technology and Applications, 11763, 1797-1802.
[3] Gutty, F., Grisard, A., Joly, A., et al. (2015) Multi-kW Peak Power Acousto-Optically Tunable Thulium-Doped Fiber Laser System. Optics Express, 23, 6754-6762.
[4] Samion, M.Z., Ismail, M.F., Muhamad, A., et al. (2016) Tunable Passively Q-Switched Thulium-Doped Fiber Laser Operating at 1.9 μm Using Arrayed Waveguide Grating (AWG). Optics Communications, 380, 195-200.
[5] Zhou, R.L., Ju, Y.L., Zhao, J., et al. (2013) A Theoretical and Experimental Investigation of an In-Band Pumped Gain-Switched Thulium-Doped Fiber Laser. Chinese Physics B, 22, 064208.
[6] Zhang, H.R., Lin, W., Wu, D.D., et al. (2021) Direct Generation of 7 W, 360 μJ Multi-Pulse Laser from an Ultracompact All-Fiber Gain Switched Tm^{3+}-Doped Double-Clad Fiber Laser. IEEE Photonics Technology Letters, 33, 1258-1261.
[7] Tang, Y.L., Yang, Y. and Xu, J.Q. (2008) High Power Tm^{3+}-Doped Fiber Lasers Tuned by a Variable Reflective Output Coupler. Research Letters in Optics, 2008, 919403.
[8] Cheng, X., Li, Z., Hou, J., et al. (2016) Gain-Switched Monolithic Fiber Laser with Ultra-Wide Tuning Range at 2 μm. Optics Express, 24, 29126-29137.
[9] Du, G.G., Li, D.J., Zhang, M., et al. (2008) LD-Pumped 6 W CW Tm^{3+}-Doped Silica Double-Cladding Fibre Laser. Chinese Physics Letters, 25, 957-959.
[10] Newburgh, G.A., Zhang, J. and Dubinskii, M. (2017) Tm-Doped Fiber Laser Resonantly Diode-Cladding-Pumped at 1620 nm. Laser Physics Letters, 14, 125101.